

Article

Climate Change and Anthropogenic Activity Co-Driven Vegetation Coverage Increase in the Three-North Shelter Forest Region of China

Menglin Li ¹, Yanbin Qin ^{1,*}, Tingbin Zhang ^{1,2}, Xiaobing Zhou ³, Guihua Yi ⁴, Xiaojuan Bie ⁴, Jingji Li ^{2,5} and Yibo Gao ⁴

¹ College of Earth Science, Chengdu University of Technology, Chengdu 610059, China

² State Environmental Protection Key Laboratory of Synergetic Control and Joint Remediation for Soil & Water Pollution, Chengdu University of Technology, Chengdu 610059, China

³ Geological Engineering Department, Montana Technological University, Butte, MT 59701, USA

⁴ College of Tourism and Urban-Rural Planning, Chengdu University of Technology, Chengdu 610059, China

⁵ College of Ecological Environment, Chengdu University of Technology, Chengdu 610059, China

* Correspondence: qinyanbin@cdut.cn

Abstract: The Three-North Shelter Forest (TNSF) program is a significant ecological safety barrier in northern China, where both climate change and anthropogenic activity contribute to the increase in vegetation coverage observed. However, comprehensive effects of these factors on vegetation have not been accurately quantified yet. This study utilized the Global Land Surface Satellite (GLASS) Advanced Very-High-Resolution Radiometer (AVHRR) Fractional Vegetation Cover (FVC) data, meteorological data, and spatial distribution of ecological engineering to analyze spatiotemporal variation of FVC and climate in the TNSF program region in China during the period 1982–2018. A partial correlation analysis and residual analysis were performed to determine the relative contribution of climate change and anthropogenic activity to the FVC and the overall effect of ecological governance. Results showed that since 1982, the average FVC in the TNSF program region was 0.201–0.253, with an average growth rate of $0.01 \cdot (10a)^{-1}$. The FVC showed a significant increase in 66.45% of the TNSF region, and will continue to increase, while only 7.02% showed a significant decrease. The coefficient of variation showed a large spatial variation, with 30.86% being in very low stability regions, mainly distributed in Inner Mongolia and the Loess Plateau. A warm and wet climate is more conducive to increasing the FVC than the warm and dry climate, and ecological engineering has the largest impact on areas with an annual accumulated precipitation greater than 300 mm. A quantitative analysis revealed that climate change and anthropogenic activity contributed to the significant increase in the FVC in 15.58% and 46.81% of the TNSF region, respectively. Therefore, ecological governance projects, such as the TNSF program, play a crucial role in enhancing the FVC in this region.

Keywords: FVC; climate change; anthropogenic activity; residual analysis; Three-North Shelter Forest Program



Citation: Li, M.; Qin, Y.; Zhang, T.; Zhou, X.; Yi, G.; Bie, X.; Li, J.; Gao, Y. Climate Change and Anthropogenic Activity Co-Driven Vegetation Coverage Increase in the Three-North Shelter Forest Region of China. *Remote Sens.* **2023**, *15*, 1509. <https://doi.org/10.3390/rs15061509>

Academic Editors: Yoshio Inoue and Francois Girard

Received: 19 December 2022

Revised: 21 February 2023

Accepted: 7 March 2023

Published: 9 March 2023



Copyright: © 2023 by the authors. Licensee MDPI, Basel, Switzerland. This article is an open access article distributed under the terms and conditions of the Creative Commons Attribution (CC BY) license (<https://creativecommons.org/licenses/by/4.0/>).

1. Introduction

As an important constituent of terrestrial ecosystems, vegetations serve as the bond linking soil, the atmosphere, and water [1–3], play a critical role in matter cycling on the Earth's surface and energy exchange, serve as an indicator of the changes in the ecological environment [4,5], and influence the balance of global ecosystems [6,7]. As revealed by remote sensing monitoring data, global greening is being promoted by the vegetation increase within the Chinese territory [8]. The vegetation increase in China also improves the regional eco-environmental status [9,10]. However, it is uncertain if such an increase in vegetation is sustainable. Therefore, it should be beneficial to analyze variation trends of vegetation coverage in China and their driving factors in order to

promote sustainable development of the terrestrial ecosystems by adjusting environmental policies, and formulating appropriate strategies [7,11,12].

The Three-North region includes the northeastern, central north, and northwestern parts of China, constitutes 13 provinces, and accounts for 42.4% of the total land area in China. It is an ecologically vulnerable area stretching over arid, semiarid, and subhumid climates. In this area, it is hard for vegetations to grow naturally due to a lack of water and soil nutrients, land deterioration, sandstorms, etc. The Chinese government has implemented the Three-North Shelter Forest (TNSF) project in an effort to change the situation [7,13]. Existing studies have shown that this project has effectively increased the regional vegetation coverage, expanded the regional greenness [14], and improved the regional ecological environment by artificially planting on a large scale to regulate the regional climate, stabilize soil and reduce the soil erosion, and increase soil nutrients [15,16]. In addition to the ecological restoration project, climate change also acts as a critical factor in controlling vegetation growth in the TNSF region [9,13]. Air temperature is considered an important meteorological factor influencing the vegetation increase in mid-latitude areas and the primary cause for the enhanced vegetation productivity and the extended growing season in high-altitude areas [17,18]. Precipitation deficits, however, restrict the growth and development of vegetations in arid and semiarid areas [19,20].

Previous studies on vegetation changes in the TNSF region mainly focused on temporal-spatial changes, driving effects of climatic factors, and impacts of anthropogenic activities. The Normalized Differential Vegetation Index (NDVI) has been widely used as a proxy to evaluate the greenness of land surface in North China [12,14], however, it can rarely reflect the difference between different vegetation coverages since it can be disturbed by soil background and tends to be saturated in dense vegetation cover [7,21]. In comparison, fractional vegetation coverage (FVC) can more accurately represent growing status and density of vegetations, alleviate the disturbance by soil background, and enhance the reliability of spatial-temporal analysis of vegetation coverage [21,22]. Among the studies related to climatic driving factors, He et al. [9] pointed out that regional vegetations can be more influenced by precipitation than air temperature, and discovered that the rising air temperature can strengthen vegetation productivity with sufficient precipitation. Hu et al. [7] explored influences of climatic factors on vegetations in the TNSF region based on Global Land Surface Satellite (GLASS) Leaf Area Index (LAI) data, and showed that the spatial pattern of regional vegetations and different levels of ecological governance are governed by the precipitation. According to research on impacts of anthropogenic activities, policy-driven multiple afforestation projects constitute the main cause for the increased vegetations observed in the TNSF region [12,23]. However, these studies did not consider impact of the ecological governance projects distributed in the TNSF region and the driving effects by the governance projects are unknown. Moreover, the understanding of the driving effects of climate change and anthropogenic activity on the vegetation in this region is very limited. Quantitatively distinguishing the influence of climate change from that of anthropogenic activity on vegetation in the TNSF region will help us to implement and evaluate of future ecological governance projects.

This study aims to understand the changing features of the FVC and the climate change in the TNSF region based on remote sensing and meteorological data, and to quantify influences by climate change and anthropogenic activity on the FVC changes. Specifically, we will investigate (1) spatial pattern and variation trends of the FVC and climate change in the TNSF region from 1982 to 2018; (2) response of the FVC to the climate change; and (3) relative contributions of climate change and anthropogenic activity to the FVC change. Results are expected to reveal the driving factors on the FVC changes in the region and to provide technical support for ecological engineering evaluation and future ecological engineering planning in the TNSF region of China.

2. Materials and Methods

2.1. Study Area

The TNSF region includes 13 provincial-level administrative regions in North China ($73^{\circ}26'–127^{\circ}50'E$, $33^{\circ}30'–50^{\circ}12'N$). The detailed plans of reforestation have been adjusted repeatedly at different implementation stages. The total constructed area in the shelter forest is 4,069,000 km² (Figure 1), which has been adopted and reported in many studies and is also the area selected for this study. The area is high in the west and low in the east with relatively complex topography. Plateaus, mountains, and hills dominate in the west, while plains dominate in the east. Annual cumulative precipitation shows a decreasing pattern from south to north and from east to west. The majority of the study area has an annual mean air temperature ranging from 2 °C to 11 °C. The primary land coverage is desert and sandy land, while meadow vegetation is mainly distributed in Inner Mongolia, Gansu, Qinghai, and Xinjiang. Cultivated vegetation is mostly located in the eastern portion of the study area, and scarcely in the Tianshan Mountains and Jungar Basin in Xinjiang. Forest and shrub clumps are primarily found in the middle and south temperate zones, growing in areas such as the Greater Khingan Mountains, Taihang Mountains, Qinling Mountains, Tianshan Mountains, and Altai Mountains. Alpine vegetation occurs mainly in the Kunlun Mountains region (Figure 2).

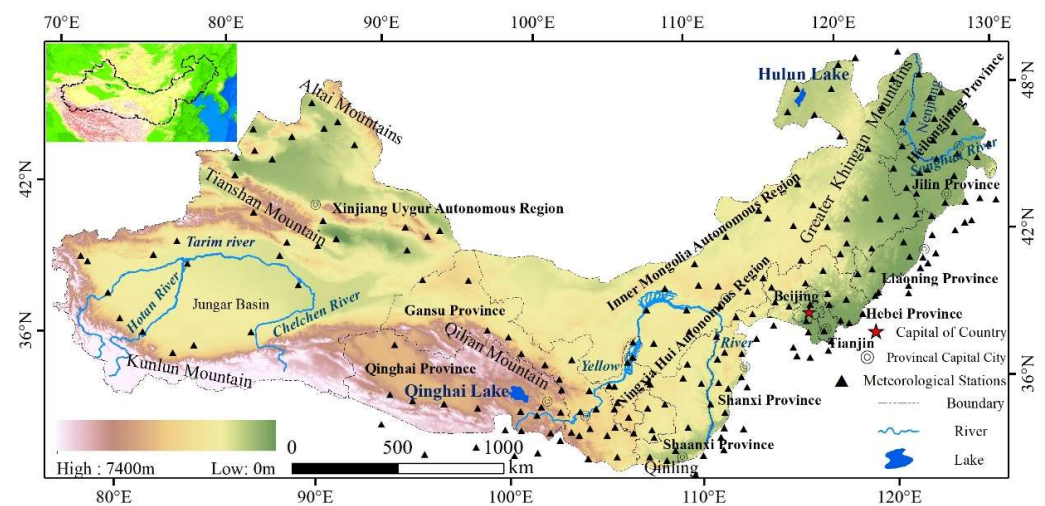


Figure 1. Elevation map in TNSF region.

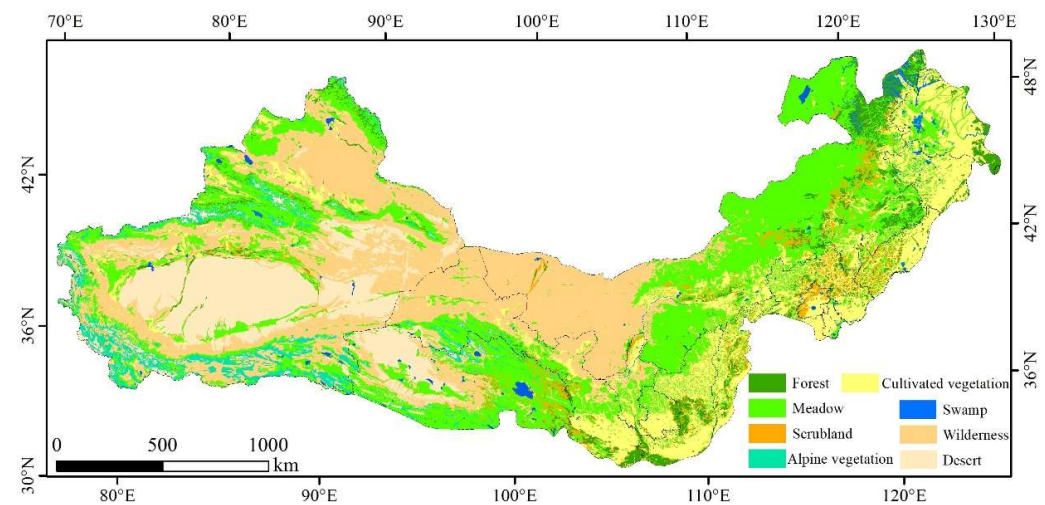


Figure 2. Vegetation types in TNSF region.

2.2. Data

The FVC data derived from the GLASS Advanced Very-High-Resolution Radiometer (AVHRR) FVC product developed by University of Maryland (<http://www.glass.umd.edu/index.html>, accessed on 10 June 2022) was produced through the multivariate adaptive regression spline method based on the AVHRR data, with a higher precision than similar products. In addition, it was featured by favorable temporal and spatial continuity [24], and its spatial resolution and temporal resolution were 5000 m and 8 d, respectively. The data products from 1982 to 2018 were converted into Geotiff format and underwent preprocessing, including reduction using a proportionality coefficient, reprojection, and clipping to the study area. Finally, the effects of the atmosphere and solar elevation were corrected using the maximum value synthesis method to obtain the interannual data of the study area.

The meteorological data used in this research came from the China Meteorological Data Service Center (<http://data.cma.cn/>, accessed on 10 June 2022). The accuracy of spatial interpolation of the meteorological data is affected by two primary factors: spatial distribution of meteorological stations and spatial interpolation method of data. Air temperature and precipitation data were collected from 217 meteorological stations over the TNSF region, which were evenly distributed. For interpolation of the precipitation data, the commonly used Inverse Distance Weighted (IDW) and Kriging methods were used in northern China [25,26]. After comparing their accuracies, the Kriging method was selected for sole use in this study. On the other hand, air temperature is closely related to altitude or topography [27]. Thus, the ANUSPLINE interpolation method that incorporates altitude as a covariate was chosen for the spatial interpolation of air temperature data [28]. The spatial resolution of the interpolated meteorological data was standardized to 5000 × 5000 m.

Vegetation type data came from the 1:1 million national vegetation type dataset published by the Resource and Environment Science and Data Center of the Chinese Academy of Sciences (<https://www.resdc.cn/data.aspx?DATAID=122>, accessed on 10 June 2022). Vegetations in the TNSF region were divided into 8 types after preprocessing, such as clipping and reprojection (Figure 2).

DEM data used were the NASADEM data provided by Google Earth Engine that were the reprocessed SRTM DEM data with a higher accuracy. (<https://earthengine.google.com/>, accessed on 10 June 2022). The data were resampled to 5000 m after preprocessing like clipping and projection.

2.3. Methods

2.3.1. Theil–Sen Trend Analysis and Mann–Kendall Statistical Test

The Theil–Sen method, a robust nonparametric trend analysis method with good noise immunity, evaluates trends and degrees by calculating the median of the data combinations' slope [29], specifically as follows:

$$\beta = \text{median}\left(\frac{x_j - x_i}{j - i}\right) (1 < i < j < n) \quad (1)$$

where β is the median value of the slope of all data if β is greater than 0, the FVC change shows an upward trend, and if $\beta < 0$, the FVC change shows a downward trend. x_i and x_j are the two variables in a time series, n is the number of years of the time series (1982–2018), i.e., $n = 37$, and median represents the median value of a series of values.

The Mann–Kendall method with a strong anti-interference performance was used to test the significance of FVC trends, and the tested samples did not need to follow certain distributions [6]. This method has been widely applied to time series analysis of

hydrological, meteorological, and vegetation indexes [30], with Z as a standard statistical variable. The formula for Z is as below:

$$z = \begin{cases} \frac{S-1}{\sqrt{\text{var}(S)}}, & S > 0 \\ 0, & S = 0 \\ \frac{S+1}{\sqrt{\text{var}(S)}}, & S < 0 \end{cases} \quad (2)$$

$$S = \sum_{i=1}^{n-1} \sum_{j=i+1}^n \text{sgn}(x_j - x_i) \quad (3)$$

$$\text{sgn}(x_j - x_i) = \begin{cases} 1 & \text{if } (x_j - x_i) > 0 \\ 0 & \text{if } (x_j - x_i) = 0 \\ -1 & \text{if } (x_j - x_i) < 0 \end{cases} \quad (4)$$

$$\text{Var}(s) = \frac{n(n-1)(2n+5)}{18} \quad (5)$$

where $\text{sgn}(x)$ is the sign functional. During a bilateral trend test, if the absolute value of Z is greater than 1.65, 1.96, and 2.58, the trend passes the significance test, and the corresponding reliability is 90%, 95%, and 99%, respectively. In this research, 95% was adopted for a reliability test. In addition, four variation trends—significant increase ($\beta > 0$, $|Z| > 1.96$), significant decrease ($\beta < 0$, $|Z| > 1.96$), slight increase ($\beta > 0$, $|Z| < 1.96$), and slight decrease ($\beta < 0$, $|Z| < 1.96$)—were obtained after considering the Theil–Sen trend analysis and Mann–Kendall test results.

2.3.2. Coefficient of Variation

Coefficient of variation is used to describe the dispersion degree of coverage, and the fluctuation of this index can reflect the FVC stability of a region [22]. The formula is as follows:

$$\text{CV}_{\text{FVC}} = \frac{1}{\overline{\text{FVC}}} \sqrt{\frac{1}{(n-1)} \sum_{i=1}^n (\text{FVC}_i - \overline{\text{FVC}})^2} \quad (6)$$

where $\overline{\text{FVC}}$ is the average of a time series of FVC_i , $i = 1, 2, 3, \dots, n$

2.3.3. Hurst Index

As a method to distinguish the sustainability of time series data, the Hurst index is widely used in hydrology, climatology, and vegetation studies [5,31]. There are several different methods for calculating this index, and it is generally believed that results of the readjust range analysis are more reliable [32]. The calculation procedure is as follows:

For a long time series:

$$\{\text{FVC}(t)\}, t = 1, 2, 3, 4 \dots n. \quad (7)$$

We define a series of the mean of the long time series as

$$\overline{\text{FVC}}_{\tau} = \frac{1}{\tau} \sum_{t=1}^{\tau} \text{FVC}_t, \tau = 1, 2, 3 \dots n. \quad (8)$$

The accumulated deviation for each mean $\overline{\text{FVC}}_{\tau}$ is calculated as below

$$X_{(t,\tau)} = \sum_{t=1}^t (\text{FVC}_t - \overline{\text{FVC}}_{\tau}) \quad 1 \leq t \leq \tau \quad (9)$$

The range sequence R is then defined as

$$R_{(\tau)} = \max_{1 \leq t \leq \tau} X_{(t,\tau)} - \min_{1 \leq t \leq \tau} X_{(t,\tau)} \quad \tau = 1, 2, 3 \dots n. \quad (10)$$

and the standard deviation sequence $S_{(\tau)}$ is defined as

$$S_{(\tau)} = \left[\frac{1}{\tau} \sum_{t=1}^{\tau} (FVC_{(t)} - FVC_{\tau})^2 \right]^{\frac{1}{2}} \tau = 1, 2, 3 \dots n \quad (11)$$

Finally, the Hurst exponent index H can be found from the following formula:

$$\frac{R_{(\tau)}}{S_{(\tau)}} = (c\tau)^H \quad (12)$$

2.3.4. Correlation Analysis

The correlation coefficient method has been extensively used to analyze the correlations between vegetation indexes and climatic factors, but simple correlation coefficients cannot accurately describe the influences of multiple climatic factors on FVC, as in the multivariate correlation analysis. On the contrary, partial correlation coefficients can accurately describe correlations between single independent variables and dependent variables [21,33]. Partial correlation coefficients are subjected to significance tests through the t test method. When $|t| > t_{0.05}$, the second-order partial correlation coefficients are considered statistically significant.

2.3.5. Residual Analysis

A residual analysis is based on the assumption that FVC is closely correlated with climatic and anthropogenic factors, and it can be used to distinguish the influence on vegetation FVC by the climate change and anthropogenic activity and their relative contributions [34]. A residual analysis was performed through the following three steps: (1) a linear regression model was established with the FVC as the dependent variable and climatic factors as independent variables; (2) predicted value FVC_{pre} was calculated based on climatic factors and a regression model to quantify the influence of climate change on the FVC; (3) the difference between the predicted value FVC_{pre} and the observed value FVC_{obr} , i.e., the residual error FVC_{res} was calculated, which indicated the influencing degree of other factors on the FVC. The regression model is expressed by the following formula:

$$FVC = a + b \times x_1 + c \times x_2 \quad (13)$$

where x_1 and x_2 denote the air temperature and precipitation, respectively; a , b , and c are coefficients. According to the residual analysis results, relative contributions of climatic factors to the FVC were then calculated as follows:

$$R_1 = \frac{\text{slope}(FVC_{pre})}{\text{slope}(FVC_{obr})} \times 100\% \quad (14)$$

The relative contribution of the anthropogenic activity to the FVC was then calculated as $R_2 = 1 - R_1$.

3. Results

3.1. Spatial-Temporal Variation Features of FVC

The FVC in the TNSF region during 1982–2018 witnessed an overall growing trend, with the annual mean value ranging from 0.201 to 0.253 (Figure 3a). Before 1998, the FVC fluctuated by a broad range of 1–2%. Afterward, interannual variation amplitude of the FVC decreased, and the average growth rate was elevated to $0.0136 \cdot (10a)^{-1}$. To more objectively reveal the temporal changes of the FVC in the TNSF region, we divided the FVC into extremely low (<0.1), low (0.1–0.29), medium (0.3–0.49), high (0.5–0.69), and extremely high (>0.7), conforming with the desertification standard specified in the Land Desertification Monitoring Method of the People's Republic of China [21]. In the past 37 years, the area with an extremely low-FVC area decreased from 2,377,200 km² in

1982 to 2,158,100 km² in 2018. The area with an extremely high-FVC showed a significant increasing trend with a net increase of 210,400 km². The area changes of other FVC types were not evident (Figure 3b).

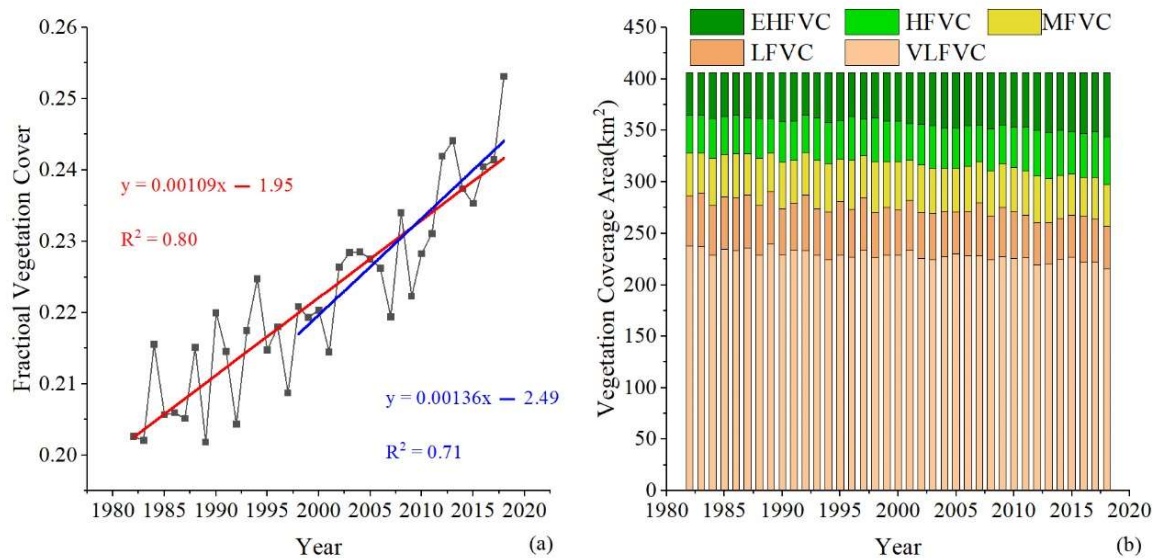


Figure 3. Interannual variation of the mean FVC (a) and area variation in different FVC types (b) in TNSF region. FVC types include VLFVC (Very Low Fractional Vegetation Cover), LFVC (Low Fractional Vegetation Cover), MVC (Medium Fractional Vegetation Coverage), HVC (High Fractional Vegetation Coverage), and EHFVC (Extremely High Fractional Vegetation Cover).

The maximum value of the annual average FVC in the TNSF region was 0.96, and the high-value areas with an FVC greater than 0.7 were mainly distributed in three provinces in northeast China (Heilongjiang, Jilin, Liaoning), the Greater Khingan Range, the east and north of Hebei, Beijing, Tianjin, Shanxi, and the middle and south of Shaanxi, the south of Gansu and Qinghai, the southeast of the Qilian Mountains, Mount Tianshan range, and the Altai Mountains. FVC in the Tianshan, Altai Mountain, Qilian Mountains, and Greater Khingan Mountains showed a decreasing trend from high altitudes to low altitudes (Figure 4). Vegetations were more susceptible to anthropogenic activities at low-altitude regions where anthropogenic activities were more intense. Restricted by natural conditions, the low-value areas with FVC < 0.1 were widely distributed in the wilderness and desert areas in the north of northwestern and northern China.

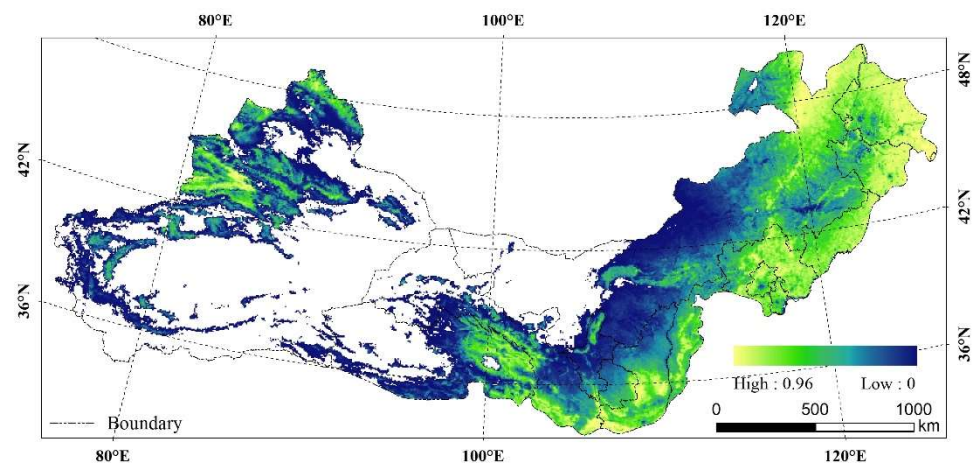


Figure 4. Spatial distribution of the multi-year average value of FVC in TNSF region.

As revealed by the Theil–Sen trend analysis and the Mann–Kendall test results, FVC changes in the TNSF region showed a significant increasing trend since 1982, with the proportion reaching 66.45% in area, and it was distributed in the whole TNSF region (Figure 5). A slight increase or decrease in FVC was observed mainly in the middle and north of Inner Mongolia, and the proportion of these two types reached about 26.26%. The area with prone to significant decreasing trends accounted for 7.29% in the TNSF region, and they showed a concentrated distribution only in Beijing, Tianjin, the three provinces in Northeast China, and the middle of the Tianshan range (Figure 5).

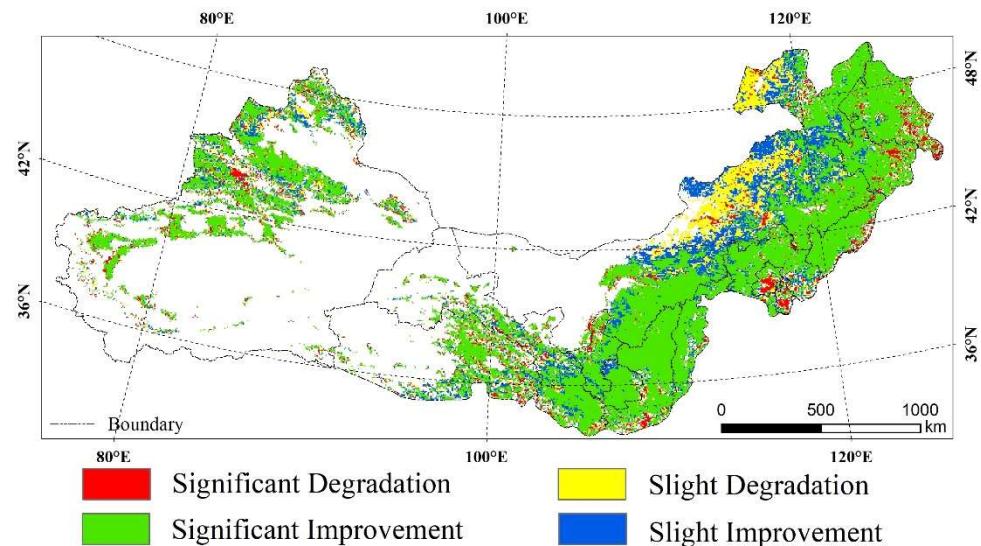


Figure 5. Spatial distribution of FVC change trend types in TNSF region.

Results of the variation coefficient analysis showed an average value of 0.3, indicating a strong fluctuation of vegetation in the TNSF region. The spatial distribution of vegetated area with extreme stability was found to be congruent with the areas of high vegetation coverage, accounting for 37.22% in area and primarily composed of cultivated vegetation, shrub, and forest covers (Figure 4). The proportion of areas with high stability was 30.86%, mostly located in Inner Mongolia, Shaanxi, Ningxia, Gansu, and Xinjiang, encompassing most of the meadow regions in the study area. Meadow lands exhibiting strong stability were predominantly located in the high-altitude region of the Qilian Mountains, Tianshan Mountains, and Altai Mountains. The coefficients of variation of other land types accounted for about 10% each (Figure 6).

The mean value of the Hurst index was found to be 0.73, indicating that the trend of the FVC variation in the TNSF region over the past 37 years is likely to persist. By combining the results of the Hurst index and Theil–Sen trend analysis, we determined the future trend of FVC in the study area. The results showed that 69% of the area displayed a trend of continuous improvement in FVC, with a distribution range similar to that of the significant improvement area (Figure 5). About 28% of the area displayed a continuous degradation trend; these areas are concentrated in central and northern Inner Mongolia, in Beijing and Tianjin, with sporadic occurrences in other regions (Figure 7). In the future, it is expected that only 1% and 2% of the region will show degradation and improvement in FVC, respectively, with no centralized distribution (Figure 7).

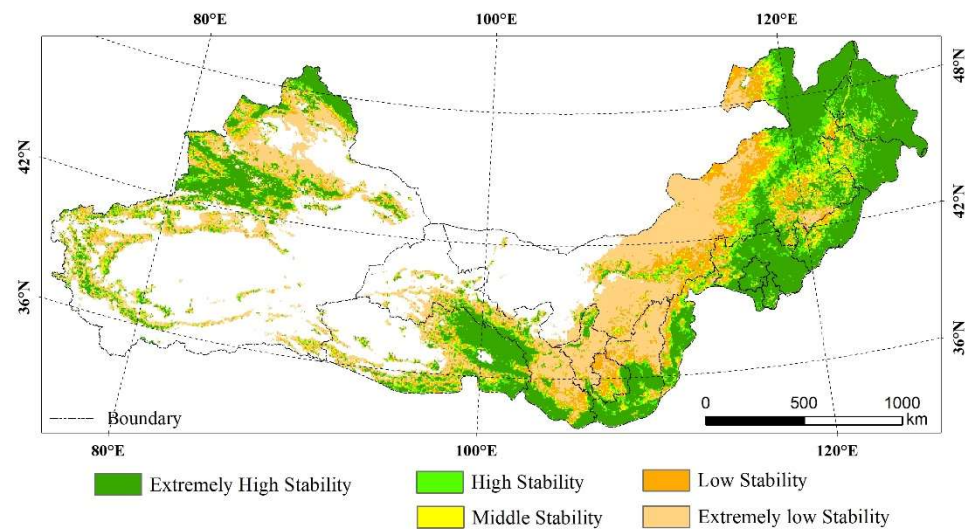


Figure 6. Spatial distribution of FVC stability in TNSF region.

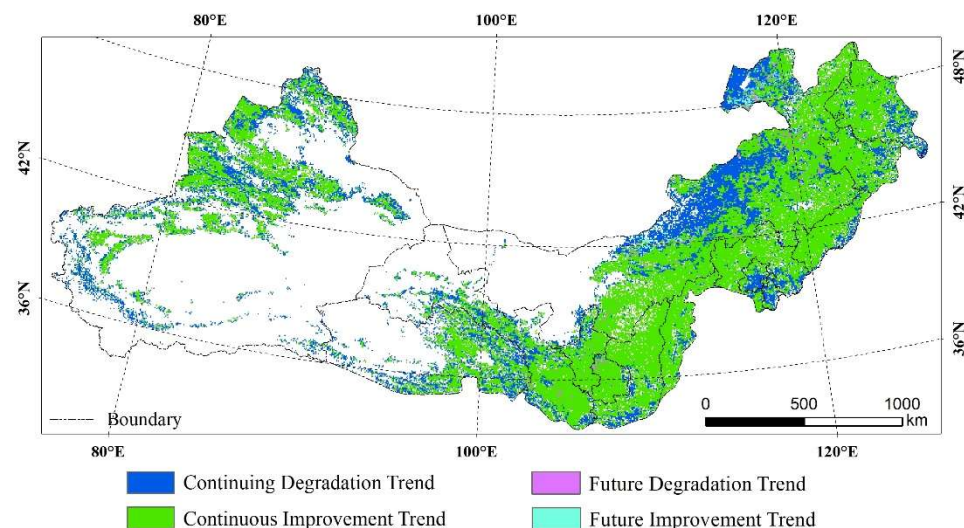


Figure 7. Spatial distribution of FVC future change trend in TNSF region.

3.2. Spatial-Temporal Characteristics of Climate Change

Over the past 37 years, the annual average temperature in the TNSF region ranged from 7.1 °C to 13.9 °C. Areas with a high temperature were mainly located in Beijing, Tianjin, the south of Shaanxi, as well as the Tarim and Turpan basins in Xinjiang, where the annual average temperature exceeded 11 °C. Areas with a low temperature mainly occurred at high-altitude localities in the Kunlun Mountains, with an annual increase in the average temperature lower than 0 °C (Figure 8). The years after 1982 witnessed a rising trend of the annual average temperature in the TNSF region; the annual maximum temperature reached 0.11 °C, and the temperature rise was the most apparent in the Kunlun Mountains and Qilian Mountains (Figure 9).

Spatial distribution of precipitation highly resembled that of the FVC, with overall rainfall decreasing from east to west (Figure 10). Areas with low-precipitation areas were mainly located in northwest China, where the annual total precipitation was less than 100 mm. Areas with a high precipitation were mainly distributed in the east of the TNSF region, where the highest precipitation was about 700 mm. Precipitation increase was the most significant in Shaanxi, Gansu, and Ningxia, as well as the south of Qinghai, and the annual precipitation decreased evidently in the northeast of the TNSF region (Figure 11).

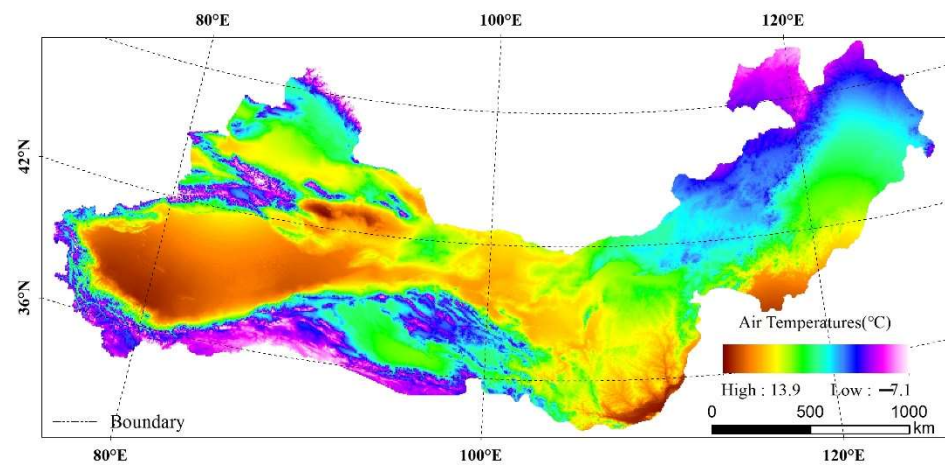


Figure 8. Spatial distribution of the air temperature in TNSF region from 1982 to 2018.

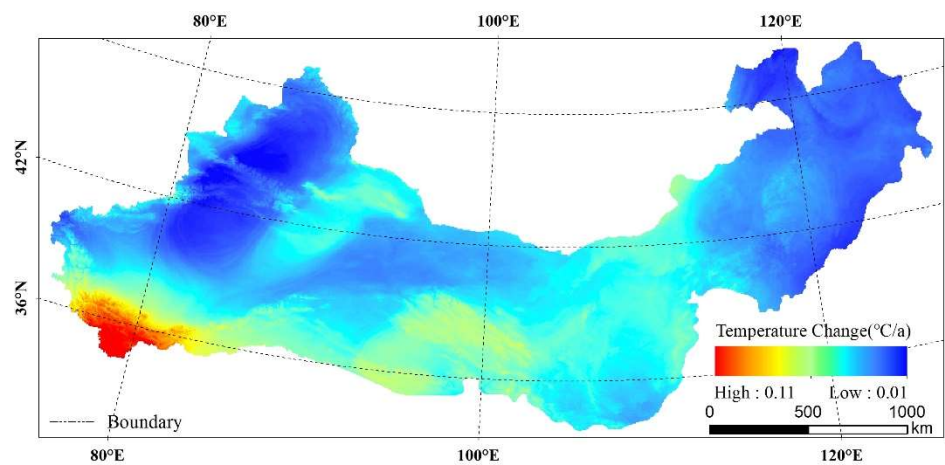


Figure 9. Spatial distribution of the air temperature variation in TNSF region from 1982 to 2018.

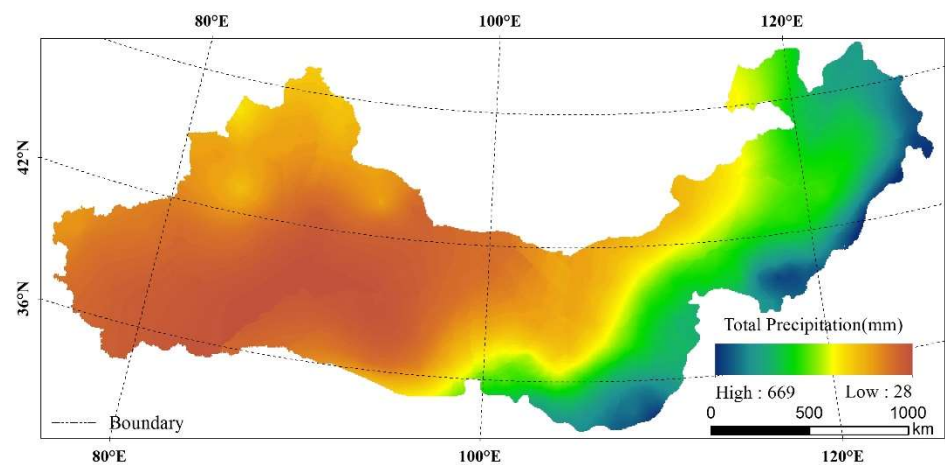


Figure 10. Spatial distribution of the precipitation in TNSF region from 1982 to 2018.

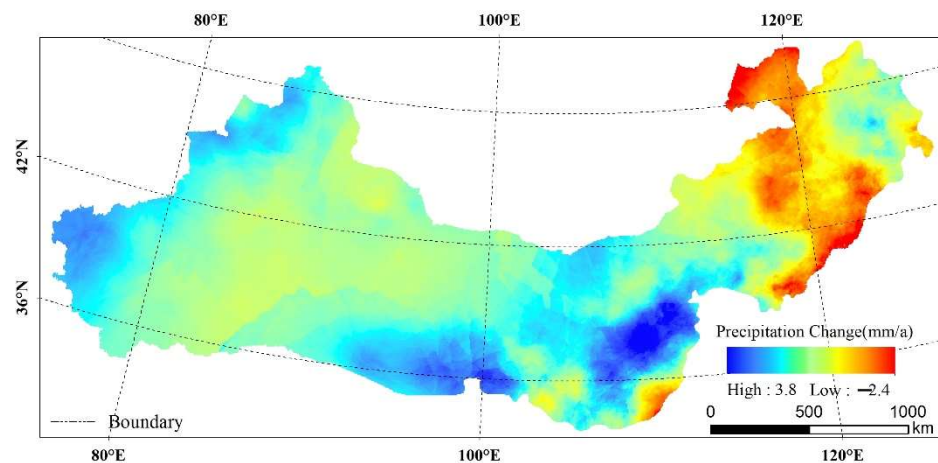


Figure 11. Spatial distribution of the precipitation variation in TNSF region from 1982 to 2018.

3.3. Response of FVC to Climate Change

According to the t test results, the areas with the absolute value greater than 0.33 in the partial correlation coefficient between the FVC and the climatic factor were considered to pass the significance test. The FVC showed significantly positive correlations with the air temperature and precipitation in 27.69% and 38.92% of the TNSF region, respectively. Specifically, the FVC was significantly positively correlated with the air temperature in the north of Hebei, the southeast of Inner Mongolia, Shaanxi, Gansu, and Ningxia, and Shanxi. However, it exhibited a significantly negative correlation with the air temperature in the middle and north of Inner Mongolia, as well as metropolitan regions such as Beijing and Tianjin (Figure 12). The partial correlation between the FVC of cultivated vegetation, shrubs, and forests and climate factors was significant and positive, while the correlation between the FVC of meadows and temperature varied by region. The relationship between the FVC of meadow lands and climate factors was mostly insignificant in Xinjiang, while in Inner Mongolia, the FVC of most of the meadow lands were negatively or significantly negatively correlated with the temperature. In contrast, the FVC of meadow lands in the Qilian Mountains displayed a significantly positive correlation with the temperature (Figure 12).

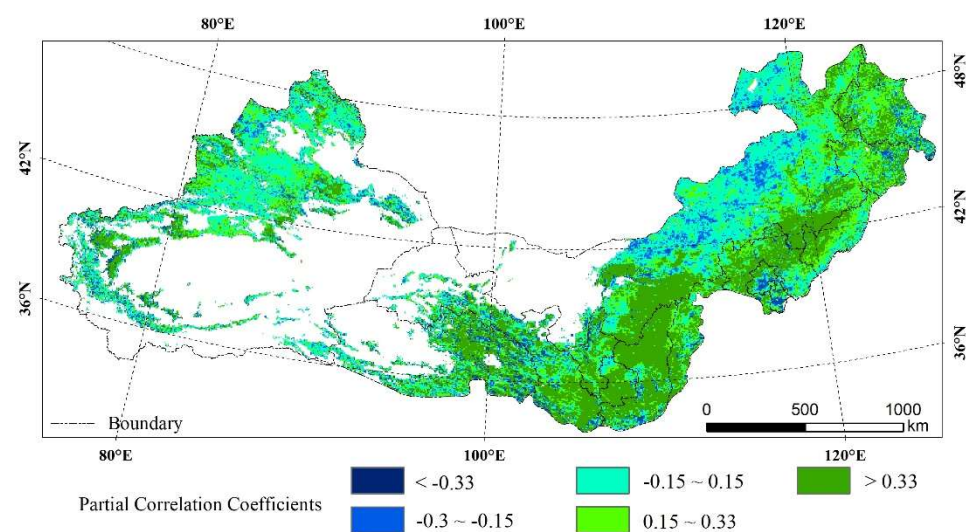


Figure 12. Spatial distribution of partial correlation coefficients between FVC and air temperature in TNSF region.

In addition, positive and negative partial correlations between FVC and precipitation accounted for 72.06% and 27.83%, respectively. Vegetation growth in the northwestern part

of the study area was generally limited by insufficient precipitation, and the cultivated vegetation and meadows in the Hulun Lake area of Inner Mongolia and the Loess Plateau responded most strongly to precipitation, showing a significant positive correlation [19]. In the east and south areas with abundant precipitation, however, excessive rainy days was not conducive to plant photosynthesis [30], and consequently, there was no significant correlation between cultivated vegetation and precipitation (Figure 13).

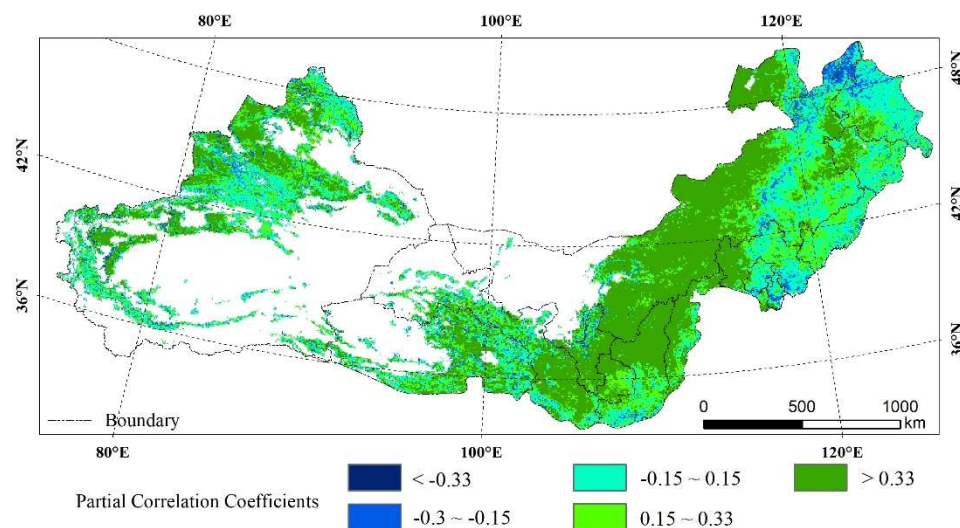


Figure 13. Spatial distribution of partial correlation coefficients between FVC and precipitation in TNSF region.

4. Discussion

4.1. Implementation Effect of Ecological Governance

Over the past 44 years, the Chinese government has implemented six major ecological governance programs in the TNSF region (Figure 14), including the Three-North Shelter Forest Development Program, the Beijing-Tianjin Sand Source Control Program (BSSCP), the Nature Forest Conservation Program (NFCP), the Sanjiangyuan Ecological Protection and Construction Program (SEPCP), the Grazing to Grassland Program (GTGP), and the Grain to Green Program (GTGP). One of the goals of these programs is to improve vegetation coverage. To achieve the goals of these programs across multiple areas, the government has adopted a phased approach and has maintained long-term substantial investment in ecological governance [7]. The Three-North Shelter Forest Program, initiated in 1978, was the first significant program carried out [35]. Over the past 40 years, a total area of 317,400 km² of forest has been preserved and afforested, providing valuable experience and technology for future large-scale ecological governance programs that began around 2000 [36]. Additional information on these programs can be found in the relevant literature [37–41].

A minimum of three ecological improvement projects have been executed in 80% of the county-level administrative regions. Regions with an implementation of 4–5 governance engineering projects are the focus of governance and are located in the Greater Hinggan Mountains, the western part of Inner Mongolia, the Loess Plateau, the Qilian Mountains, the Sanjiangyuan and the Tian Shan, Altai Mountains and Kunlun Mountains in Xinjiang. With more ecological engineering projects being implemented in the region and more comprehensive governance measures in place, the trend of improving vegetation coverage was more obvious. However, with an increase in governance projects, the proportion of areas where anthropogenic activity significantly increased FVC showed a decreasing trend, which indicated that the governance of focus areas was extremely challenging (Table 1). Furthermore, the increase in surface vegetation coverage is strongly correlated with the capital investment in ecological engineering [7,41].

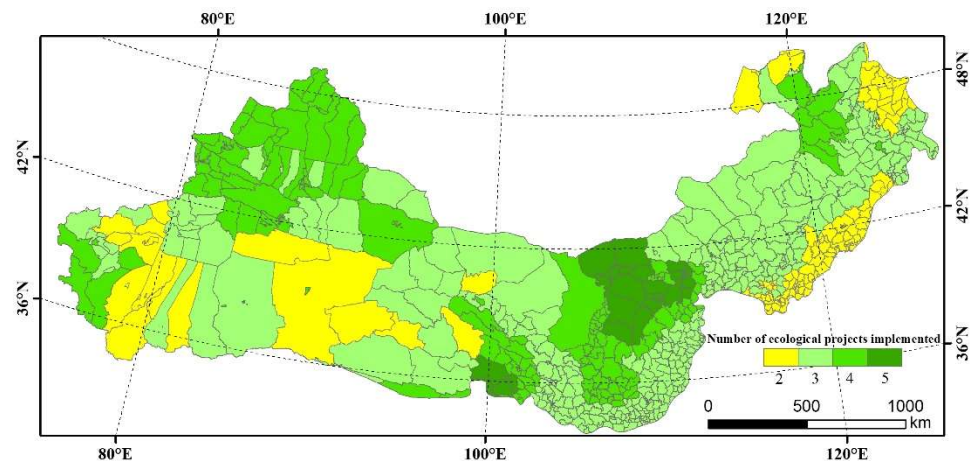


Figure 14. Locations of the quantity of ecological governance projects in TNSF region.

Table 1. Proportion of different types of driving factors in the ecological superposition area.

Spatial Pattern Types	Two Programs	Three Programs	Four Programs	Five Programs
CCSFD	2.07%	1.50%	2.45%	1.84%
CFSFD	0.75%	0.51%	0.71%	0.78%
AASFD	6.67%	4.70%	4.28%	0.52%
CCSD	4.74%	2.41%	1.06%	0.80%
CFSD	1.07%	0.92%	0.36%	0.33%
AASD	1.99%	5.26%	2.30%	0.97%
AASI	2.82%	7.24%	7.00%	4.84%
CFSI	0.59%	1.38%	1.46%	1.18%
CCSI	1.26%	3.88%	5.02%	3.85%
AASFI	63.55%	47.99%	41.75%	29.57%
CFSFI	4.57%	10.88%	14.30%	29.33%
CCSFI	9.92%	13.32%	19.32%	26.00%

Note: (CCSFI) Climate Change-Induced Significant Increase, (CFSFI) Comprehensive Factor-Induced Significant Increase, (AASFI) Anthropogenic Activity-Induced Significant Increase, (CCSI) Climate Change-Induced Slight Increase, (CFSI) Comprehensive Factor-Induced Slight Increase, (AASI) Anthropogenic Activity-Induced Slight Increase, (CCSD) Climate Change induced Slight Decrease, (CFSD) Comprehensive Factor-Induced Slight Decrease, (AASD) Anthropogenic Activity-Induced Slight Decrease, (CCSFD) Climate Change Induced Significant Decrease, (CFSFD) Comprehensive Factor-Induced Significant Decrease, (AASFD) Anthropogenic Activity-Induced Significant Decrease.

4.2. FVC Variation Drives Quantitative Analysis and Spatial Differences

The relative contributions of climatic factors and anthropogenic activities to the FVC in the TNSF region were calculated based on residual analysis results. In this research, contribution rates greater than 55% were defined as the driving factors of climate change or anthropogenic activity, and 45–55% were defined as comprehensive driving factors. Moreover, relative contributions and FVC variation trend types were superposed to acquire 12 driving types, aiming to intuitively distinguish the spatial distribution of climate change and anthropogenic activity-driven FVC in the TNSF region since 1982 (Figure 15). The results indicated that vegetation increased in 86.4% of the TNSF region, with 74.86% of these areas showing a significant increase (Table 2). Areas with a significant increase in vegetation driven by anthropogenic activity were the most widely distributed (about 46.81% of the total area).

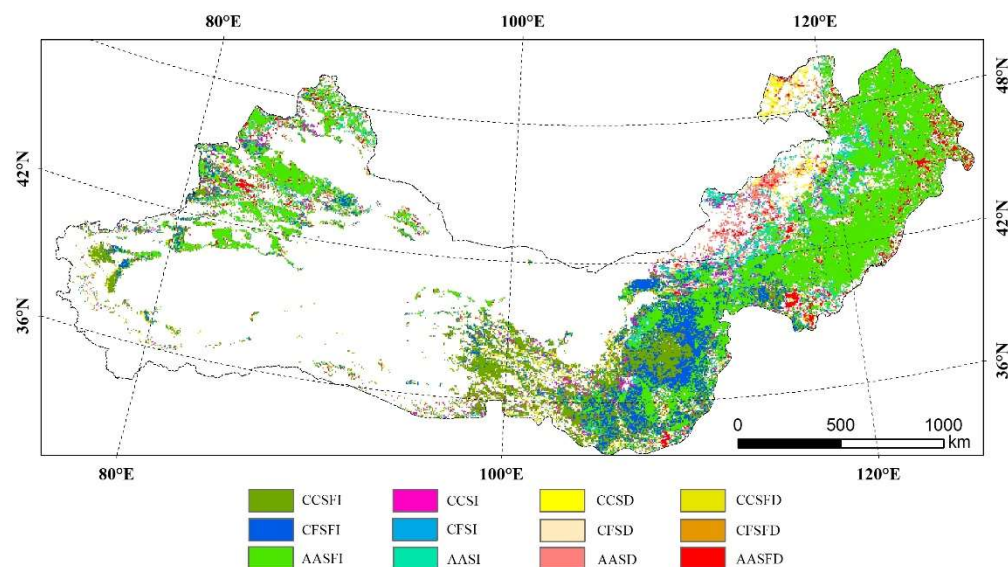


Figure 15. Spatial patterns of the effect of climate change and anthropogenic activity on the vegetation dynamics in the TNSF region. Spatial pattern types: (CCSFI) Climate Change-Induced Significant Increase, (CFSFI) Comprehensive Factor-Induced Significant Increase, (AASFI) Anthropogenic Activity-Induced Significant Increase, (CCSI) Climate Change-Induced Slight Increase, (CFSI) Comprehensive Factor-Induced Slight Increase, (AASI) Anthropogenic Activity-Induced Slight Increase, (CCSD) Climate Change induced Slight Decrease, (CFSI) Comprehensive Factor-Induced Slight Decrease, (AASD) Anthropogenic Activity-Induced Slight Decrease, (CCSFD) Climate Change Induced Significant Decrease, (CFSFD) Comprehensive Factor-Induced Significant Decrease, (AASFD) Anthropogenic Activity-Induced Significant Decrease.

Table 2. Driving factors of FVC and its areal proportion.

Types of Driving Factors	Proportion (%)	Types of Driving Factors	Proportion (%)
Climate Change-Induced Significant Increase (CCSFI)	15.58	Climate Change-Induced Significant Decrease (CCSFD)	1.88
Comprehensive Factor-Induced Significant Increase (CFSFI)	12.47	Comprehensive Factor-Induced Significant Decrease (CFSFD)	0.62
Anthropogenic Activity-Induced Significant Increase (AASFI)	46.81	Anthropogenic Activity-Induced Significant Decrease (AASFD)	4.53
Climate Change-Induced Slight Increase (CCSI)	3.85	Climate Change-Induced Slight Decrease (CCSD)	2.20
Comprehensive Factor-Induced Slight Increase (CFSI)	1.29	Comprehensive Factor-Induced Slight Decrease (CFSI)	0.73
Anthropogenic Activity-Induced Slight Increase (AASI)	6.40	Anthropogenic Activity-Induced Slight Decrease (AASD)	3.64

From a spatial distribution perspective, governance engineering has performed well in the northeastern plains, the Loess Plateau, and some areas of Xinjiang (Figure 14). The effect is closely tied to the distribution of climate patterns [9,42]. The significant increase in the vegetation coverage driven by anthropogenic activity and is also closely related to the distribution of climatic patterns, indicating a synergy between the climate change and

anthropogenic actions. In the northeastern plains and Loess Plateau, there are generally two to three governance projects, and areas with significant increase in vegetation coverage are mainly located in regions with more than 300 mm of precipitation. Adequate rainfall supports the effectiveness of tree planting, reforestation, and grassland protection [7]. In Xinjiang, where the annual precipitation is far less than 300 mm, the growth of vegetation mainly depends on the water source from snow and ice melting [43,44]. At the same time, temperature and precipitation in the region are increasing, and the ecological governance of the warm and moist climate has achieved good results [7,45]. Three ecological governance projects have been implemented in the central and northern part of Inner Mongolia, but the implementation effect was poorer. This is mainly due to the obvious decrease in precipitation, while the temperature showed a rising trend. Therefore, the warm and dry climate has led to a possible degradation trend of FVC in parts of Inner Mongolia [46], which has increased the challenge of ecological governance [47]. In addition, as the grasslands are most extensively distributed in China, overgrazing by the animal husbandry may have also caused the degradation of grasslands [48].

In the future, implementation of new ecological governance projects in the TNSF region should take into account the regional climate pattern. Large-scale ecological governance in areas with annual cumulative precipitation less than 300 mm may not be suitable effective [40]. Areas such as Xinjiang that have achieved positive results, but excessive planting of trees and grass and increased cultivation of vegetation may accelerate consumption of water resources and may cause water shortage [49–51]. Implementation of any ecological governance in areas with precipitation above 300 mm may benefit from previous experience in gaining the greatest ecological outcomes.

5. Conclusions

The interannual spatial-temporal changes of the FVC in the TNSF region from 1982 to 2018 were analyzed, and the main driving factors were identified, which sparked new insight into the regional FVC increase or decrease and the underlying cause. The results showed that the FVC in the TNSF region of China exhibited a spatial distribution pattern of increasing from the west to the east. Spatially, the FVC was significantly improved, and the multi-year average value showed a growing trend. The implementation of six national-level ecological governance projects had a positive impact, and anthropogenic activity was found to significantly contribute to the FVC improvement in 46.81% of the TNSF region. With a greater number of ecological projects implemented, a greater areal proportion of FVC improvement was found. Climate change affects the effectiveness of ecological governance projects to a certain degree. A warm and humid climate is more conducive to the FVC increase than a warm and dry climate. Ecological governance projects implemented in areas with an annual cumulative precipitation above 300 mm are more effective than those implemented in areas with less precipitation. Regional water resource capacity should be considered when implementing any ecological governance in low-precipitation areas. It is expected that TNSF region restoration projects should be continuously encouraged to ensure sustainable vegetation improvement if the synergy between climate change and anthropogenic activity is considered.

Author Contributions: Conceptualization, M.L.; Formal analysis, Y.Q.; Funding acquisition, T.Z. and G.Y.; Methodology, G.Y. and X.Z.; Software, M.L.; Supervision, Y.Q.; Validation, X.B. and X.Z.; Visualization, J.L.; Writing—original draft, M.L.; Writing—review and editing, Y.Q., T.Z. and Y.G. All authors have read and agreed to the published version of the manuscript.

Funding: This research was funded by the National Natural Science Foundation of China (41801099), the second Tibetan Plateau Scientific Expedition and Research Program (2019QZKK0307), and the Key Research and Development Program of Sichuan (2022YFS0491).

Data Availability Statement: The GLASS data are available at Global Land Surface Satellite (GLASS) (umd.edu), accessed on 10 June 2022. The meteorological data are available at <http://data.cma.cn/>, accessed on 10 June 2022. The vegetation types are available at <https://www.resdc.cn/data.aspx?>

DATAID=122, accessed on 10 June 2022. The DEM are available at <https://earthengine.google.com/>, accessed on 10 June 2022.

Conflicts of Interest: The authors declare no conflict of interest.

References

- Gerten, D.; Schaphoff, S.; Haberlandt, U.; Lucht, W.; Sitch, S. Terrestrial Vegetation and Water Balance—Hydrological Evaluation of a Dynamic Global Vegetation Model. *J. Hydrol.* **2004**, *286*, 249–270. [[CrossRef](#)]
- Ahlström, A.; Xia, J.; Arneeth, A.; Luo, Y.; Smith, B. Erratum: Importance of Vegetation Dynamics for Future Terrestrial Carbon Cycling. *Environ. Res. Lett.* **2015**, *10*, 054019. [[CrossRef](#)]
- Duveiller, G.; Hooker, J.; Cescatti, A. The Mark of Vegetation Change on Earth’s Surface Energy Balance. *Nat. Commun.* **2018**, *9*, 679. [[CrossRef](#)] [[PubMed](#)]
- Cai, Y.; Zhang, F.; Duan, P.; Yung Jim, C.; Weng Chan, N.; Shi, J.; Liu, C.; Wang, J.; Bahtebay, J.; Ma, X. Vegetation Cover Changes in China Induced by Ecological Restoration-Protection Projects and Land-Use Changes from 2000 to 2020. *CATENA* **2022**, *217*, 106530. [[CrossRef](#)]
- Jiang, L.; Jiapaer, G.; Bao, A.; Guo, H.; Ndayisaba, F. Vegetation Dynamics and Responses to Climate Change and Human Activities in Central Asia. *Sci. Total Environ.* **2017**, *599–600*, 967–980. [[CrossRef](#)]
- Jiang, W.; Yuan, L.; Wang, W.; Cao, R.; Zhang, Y.; Shen, W. Spatio-Temporal Analysis of Vegetation Variation in the Yellow River Basin. *Ecol. Indic.* **2015**, *51*, 117–126. [[CrossRef](#)]
- Hu, Y.; Li, H.; Wu, D.; Chen, W.; Zhao, X.; Hou, M.; Li, A.; Zhu, Y. LAI-Indicated Vegetation Dynamic in Ecologically Fragile Region: A Case Study in the Three-North Shelter Forest Program Region of China. *Ecol. Indic.* **2021**, *120*, 106932. [[CrossRef](#)]
- Chen, C.; Park, T.; Wang, X.; Piao, S.; Xu, B.; Chaturvedi, R.K.; Fuchs, R.; Brovkin, V.; Ciais, P.; Fensholt, R.; et al. China and India Lead in Greening of the World through Land-Use Management. *Nat. Sustain.* **2019**, *2*, 122–129. [[CrossRef](#)] [[PubMed](#)]
- He, B.; Chen, A.; Wang, H.; Wang, Q. Dynamic Response of Satellite-Derived Vegetation Growth to Climate Change in the Three North Shelter Forest Region in China. *Remote Sens.* **2015**, *7*, 9998–10016. [[CrossRef](#)]
- Liu, X.; Xin, L. China’s Deserts Greening and Response to Climate Variability and Human Activities. *PLoS ONE* **2021**, *16*, e0256462. [[CrossRef](#)]
- Li, H.; Xu, F.; Li, Z.; You, N.; Zhou, H.; Zhou, Y.; Chen, B.; Qin, Y.; Xiao, X.; Dong, J. Forest Changes by Precipitation Zones in Northern China after the Three-North Shelterbelt Forest Program in China. *Remote Sens.* **2021**, *13*, 543. [[CrossRef](#)]
- Song, W.; Feng, Y.; Wang, Z. Ecological Restoration Programs Dominate Vegetation Greening in China. *Sci. Total Environ.* **2022**, *848*, 157729. [[CrossRef](#)] [[PubMed](#)]
- Huang, S.; Kong, J. Assessing Land Degradation Dynamics and Distinguishing Human-Induced Changes from Climate Factors in the Three-North Shelter Forest Region of China. *ISPRS Int. J. Geo-Inf.* **2016**, *5*, 158. [[CrossRef](#)]
- Zhang, Y.; Peng, C.; Li, W.; Tian, L.; Zhu, Q.; Chen, H.; Fang, X.; Zhang, G.; Liu, G.; Mu, X.; et al. Multiple Afforestation Programs Accelerate the Greenness in the “Three North” Region of China from 1982 to 2013. *Ecol. Indic.* **2015**, *61*, 404–412. [[CrossRef](#)]
- Gao, H.; Huang, Y. Impacts of the Three-North Shelter Forest Program on the Main Soil Nutrients in Northern Shaanxi China: A Meta-Analysis. *For. Ecol. Manag.* **2020**, *458*, 117808. [[CrossRef](#)]
- Ji, C.; Li, X.; Jia, Y.; Wang, L. Dynamic Assessment of Soil Water Erosion in the Three-North Shelter Forest Region of China from 1980 to 2015. *Eurasian Soil Sci.* **2018**, *51*, 1533–1546. [[CrossRef](#)]
- Sun, R.; Chen, S.; Su, H. Climate Dynamics of the Spatiotemporal Changes of Vegetation Ndvi in Northern China from 1982 to 2015. *Remote Sens.* **2021**, *13*, 187. [[CrossRef](#)]
- Ding, M.J.; Zhang, Y.L.; Sun, X.M.; Liu, L.S.; Wang, Z.F.; Bai, W.Q. Spatiotemporal Variation in Alpine Grassland Phenology in the Qinghai-Tibetan Plateau from 1999 to 2009. *Chin. Sci. Bull.* **2013**, *58*, 396–405. [[CrossRef](#)]
- Tong, S.; Zhang, J.; Ha, S.; Lai, Q.; Ma, Q. Dynamics of Fractional Vegetation Coverage and Its Relationship with Climate and Human Activities in Inner Mongolia, China. *Remote Sens.* **2016**, *8*, 776. [[CrossRef](#)]
- Ukkola, A.M.; De Kauwe, M.G.; Roderick, M.L.; Burrell, A.; Lehmann, P.; Pitman, A.J. Annual Precipitation Explains Variability in Dryland Vegetation Greenness Globally but Not Locally. *Glob. Chang. Biol.* **2021**, *27*, 4367–4380. [[CrossRef](#)]
- Li, X.; Zhang, X.; Xu, X. Precipitation and Anthropogenic Activities Jointly Green the China–Mongolia–Russia Economic Corridor. *Remote Sens.* **2022**, *14*, 187. [[CrossRef](#)]
- Liu, C.; Zhang, X.; Wang, T.; Chen, G.; Zhu, K.; Wang, Q.; Wang, J. Detection of Vegetation Coverage Changes in the Yellow River Basin from 2003 to 2020. *Ecol. Indic.* **2022**, *138*, 108818. [[CrossRef](#)]
- Niu, Q.; Xiao, X.; Zhang, Y.; Qin, Y.; Dang, X.; Wang, J.; Zou, Z.; Doughty, R.B.; Brandt, M.; Tong, X.; et al. Ecological Engineering Projects Increased Vegetation Cover, Production, and Biomass in Semiarid and Subhumid Northern China. *Land Degrad. Dev.* **2019**, *30*, 1620–1631. [[CrossRef](#)]
- Jia, K.; Yang, L.; Liang, S.; Xiao, Z.; Zhao, X.; Yao, Y.; Zhang, X.; Jiang, B.; Liu, D. Long-Term Global Land Surface Satellite (GLASS) Fractional Vegetation Cover Product Derived From MODIS and AVHRR Data. *IEEE J. Sel. Top. Appl. Earth Obs. Remote Sens.* **2019**, *12*, 508–518. [[CrossRef](#)]
- Zhang, X.; Liu, L.; Zhang, Z.; Kang, Z.; Tian, H.; Wang, T.; Chen, H. Spatial and Temporal Variation Characteristics of Glacier Resources in Xinjiang over the Past 50 Years. *Water* **2022**, *14*, 1057. [[CrossRef](#)]

26. He, D.; Yi, G.; Zhang, T.; Miao, J.; Li, J.; Bie, X. Temporal and Spatial Characteristics of EVI and Its Response to Climatic Factors in Recent 16 Years Based on Grey Relational Analysis in Inner Mongolia Autonomous Region, China. *Remote Sens.* **2018**, *10*, 961. [[CrossRef](#)]
27. Xu, Y.; Zhao, P.; Si, D.; Cao, L.; Wu, X.; Zhao, Y.; Liu, N. Development and Preliminary Application of a Gridded Surface Air Temperature Homogenized Dataset for China. *Theor. Appl. Climatol.* **2020**, *139*, 505–516. [[CrossRef](#)]
28. Luo, H.; Bie, X.; Yi, G.; Zhou, X.; Zhang, T.; Li, J.; Lai, P. Dominant Impacting Factors on Water-Use Efficiency Variation in Inner Mongolia from 2001 to 2018: Vegetation or Climate? *Remote Sens.* **2022**, *14*, 4541. [[CrossRef](#)]
29. Ren, Z.; Tian, Z.; Wei, H.; Liu, Y.; Yu, Y. Spatiotemporal Evolution and Driving Mechanisms of Vegetation in the Yellow River Basin, China during 2000–2020. *Ecol. Indic.* **2022**, *138*, 108832. [[CrossRef](#)]
30. Yuan, J.; Xu, Y.; Xiang, J.; Wu, L.; Wang, D. Spatiotemporal Variation of Vegetation Coverage and Its Associated Influence Factor Analysis in the Yangtze River Delta, Eastern China. *Environ. Sci. Pollut. Res.* **2019**, *26*, 32866–32879. [[CrossRef](#)]
31. Koutsoyiannis, D. Climate Change, the Hurst Phenomenon, and Hydrological Statistics. *Hydrol. Sci. J.* **2003**, *48*, 3–24. [[CrossRef](#)]
32. Li, S.; Wang, J.; Zhang, M.; Tang, Q. Characterizing and Attributing the Vegetation Coverage Changes in North Shanxi Coal Base of China from 1987 to 2020. *Resour. Policy* **2021**, *74*, 102331. [[CrossRef](#)]
33. Sun, Y.L.; Shan, M.; Pei, X.R.; Zhang, X.K.; Yang, Y.L. Assessment of the Impacts of Climate Change and Human Activities on Vegetation Cover Change in the Haihe River Basin, China. *Phys. Chem. Earth* **2020**, *115*, 102834. [[CrossRef](#)]
34. Chu, H.; Venevsky, S.; Wu, C.; Wang, M. NDVI-Based Vegetation Dynamics and Its Response to Climate Changes at Amur-Heilongjiang River Basin from 1982 to 2015. *Sci. Total Environ.* **2019**, *650*, 2051–2062. [[CrossRef](#)]
35. Jiao, J.; Zhang, Z.; Bai, W.; Jia, Y.; Wang, N. Assessing the Ecological Success of Restoration by Afforestation on the Chinese Loess Plateau. *Restor. Ecol.* **2012**, *20*, 240–249. [[CrossRef](#)]
36. Zhai, J.; Wang, L.; Liu, Y.; Wang, C.; Mao, X. Assessing the Effects of China’s Three-North Shelter Forest Program over 40 Years. *Sci. Total Environ.* **2023**, *857*, 159354. [[CrossRef](#)]
37. Zhao, Y.; Chi, W.; Kuang, W.; Bao, Y.; Ding, G. Ecological and Environmental Consequences of Ecological Projects in the Beijing–Tianjin Sand Source Region. *Ecol. Indic.* **2020**, *112*, 106111. [[CrossRef](#)]
38. Zhai, X.; Liang, X.; Yan, C.; Xing, X.; Jia, H.; Wei, X.; Feng, K. Vegetation Dynamic Changes and Their Response to Ecological Engineering in the Sanjiangyuan Region of China. *Remote Sens.* **2020**, *12*, 4035. [[CrossRef](#)]
39. Yuan-jie, D.; Shun-bo, Y.; Meng-yang, H.; Tong-yue, Z.; Ya-nan, L.; Zhi-wen, G.; Yi-fei, W. Assessing the Effects of the Green for Grain Program on Ecosystem Carbon Storage Service by Linking the InVEST and FLUS Models: A Case Study of Zichang County in Hilly and Gully Region of Loess Plateau. *J. Nat. Resour.* **2020**, *35*, 826. [[CrossRef](#)]
40. Shao, Q.; Liu, S.; Ning, J.; Liu, G.; Yang, F.; Zhang, X.; Niu, L.; Huang, H.; Fan, J.; Liu, J. Assessment of Ecological Benefits of Key National Ecological Projects in China in 2000–2019 Using Remote Sensing. *Acta Geogr. Sin.* **2022**, *77*, 2133–2153. [[CrossRef](#)]
41. Zhu, J.J.; Zheng, X. The Prospects of Development of the Three-North Afforestation Program (TNAP): On the Basis of the Results of the 40-Year Construction General Assessment of the TNAP. *Chin. J. Ecol.* **2019**, *38*, 1600–1610.
42. Xue, J.; Wang, Y.; Teng, H.; Wang, N.; Li, D.; Peng, J.; Biswas, A.; Shi, Z. Dynamics of Vegetation Greenness and Its Response to Climate Change in Xinjiang over the Past Two Decades. *Remote Sens.* **2021**, *13*, 4063. [[CrossRef](#)]
43. Shen, Y.J.; Shen, Y.; Guo, Y.; Zhang, Y.; Pei, H.; Brenning, A. Review of Historical and Projected Future Climatic and Hydrological Changes in Mountainous Semiarid Xinjiang (Northwestern China), Central Asia. *Catena* **2020**, *187*, 104343. [[CrossRef](#)]
44. Yao, J.; Mao, W.; Chen, J.; Dilinuer, T. Recent Signal and Impact of Wet-to-Dry Climatic Shift in Xinjiang, China. *J. Geogr. Sci.* **2021**, *31*, 1283–1298. [[CrossRef](#)]
45. Yu, H.; Bian, Z.; Mu, S.; Yuan, J.; Chen, F. Effects of Climate Change on Land Cover Change and Vegetation Dynamics in Xinjiang, China. *Int. J. Environ. Res. Public Health* **2020**, *17*, 4865. [[CrossRef](#)]
46. Li, Z.; Ma, W.; Liang, C.; Liu, Z.; Wang, W.; Wang, L. Long-Term Vegetation Dynamics Driven by Climatic Variations in the Inner Mongolia Grassland: Findings from 30-Year Monitoring. *Landsc. Ecol.* **2015**, *30*, 1701–1711. [[CrossRef](#)]
47. Li, C.; Wang, J.; Hu, R.; Yin, S.; Bao, Y.; Ayal, D.Y. Relationship between Vegetation Change and Extreme Climate Indices on the Inner Mongolia Plateau, China, from 1982 to 2013. *Ecol. Indic.* **2018**, *89*, 101–109. [[CrossRef](#)]
48. Guo, C.; Zhao, D.; Zheng, D.; Zhu, Y. Effects of Grazing on the Grassland Vegetation Community Characteristics in Inner Mongolia. *J. Resour. Ecol.* **2021**, *12*, 319–331. [[CrossRef](#)]
49. Li, M.Y.; Fang, L.D.; Duan, C.Y.; Cao, Y.; Yin, H.; Ning, Q.R.; Hao, G.Y. Greater Risk of Hydraulic Failure Due to Increased Drought Threatens Pine Plantations in Horqin Sandy Land of Northern China. *For. Ecol. Manag.* **2020**, *461*, 117980. [[CrossRef](#)]
50. Jiang, C.; Liu, J.; Zhang, H.; Zhang, Z.; Wang, D. China’s Progress towards Sustainable Land Degradation Control: Insights from the Northwest Arid Regions. *Ecol. Eng.* **2019**, *127*, 75–87. [[CrossRef](#)]
51. Zhao, R.; Liu, X.; Dong, J.; Zhao, G.; Manevski, K.; Andersen, M.N.; Tang, Q. Human Activities Modulate Greening Patterns: A Case Study for Southern Xinjiang in China Based on Long Time Series Analysis. *Environ. Res. Lett.* **2022**, *17*, 044012. [[CrossRef](#)]

Disclaimer/Publisher’s Note: The statements, opinions and data contained in all publications are solely those of the individual author(s) and contributor(s) and not of MDPI and/or the editor(s). MDPI and/or the editor(s) disclaim responsibility for any injury to people or property resulting from any ideas, methods, instructions or products referred to in the content.